Analytical description of the charge-to-photon conversion efficiency for electroluminescent devices based on thermally activated delayed fluorescence

Yungui Li[*] and Paul W. M. Blom[†]

Max Planck Institute for Polymer Research, Ackermannweg 10, 55128 Mainz, Germany

(Received 16 September 2023; revised 21 March 2024; accepted 29 March 2024; published 19 April 2024)

The efficiency of electroluminescent devices based on thermally activated delayed fluorescence (TADF) is a complex interplay of spin-allowed radiative and nonradiative singlet and triplet recombination as well as spin-flip (reverse) intersystem crossing processes. An analytical description of exciton dynamics based on the various singlet and triplet transition rates would strongly facilitate the evaluation of the effects of different processes on device performance. We present unified and analytical expressions for the exciton densities, photoluminescence quantum yield (PLQY), and charge-to-photon (CTP) conversion efficiency in TADF-based electroluminescent devices. The derivation is based on a three-level model that can also be applied to conventional fluorescence- or phosphorescence-based devices. The model allows us to analytically calculate the fundamental kinetic rates in TADF systems as well as the CTP efficiency in devices with only PLQY and transient photoluminescence decay as experimental inputs. Evaluation of the individual kinetic processes reveals that TADF emitters with PLQY as high as around 90% that exhibit pronounced delayed fluorescence, intuitively treated as potential candidates for high-performance electroluminescent devices, can still result in a CTP efficiency of only 50%–60% due to the direct competition between triplet recombination and reverse intersystem crossing.

DOI: 10.1103/PhysRevApplied.21.044037

I. INTRODUCTION

Organic luminescent semiconductors have been successfully applied for different kinds of organic electroluminescent devices, such as organic light-emitting diodes (OLEDs), organic light-emitting transistors, and electrochemical cells [1–3]. The charge transport is typically governed by a hopping mechanism, which has been experimentally verified and theoretically described by a unified extended Gaussian disorder model [4,5]. The proportion of generated excitons of different spins under electrical excitation, i.e., singlets and triplets, is a ratio of 1:3 in OLEDs, intrinsically determined by the spin of charge carriers after bimolecular recombination [6,7]. Therefore, the kinetic behavior of singlets and triplets plays different roles in device performance [8,9].

Organic luminescent materials with different emissive properties have been widely applied for organic electroluminescent devices, with either only the singlet radiative transition as prompt and conventional fluorescence, heavy-atom-assisted triplet radiation as phosphorescence, or singlet-triplet cycling as thermally activated delayed fluorescence (TADF) [3,10–12]. Because of dark processes such as intrinsic molecular relaxation or aggregation-induced quenching or trapping, the photoluminescence quantum yield (PLQY) and the charge-to-photon (CTP) efficiency in the electroluminescent devices can hardly reach unity, especially for red or near-infrared emitters in which nonradiative losses are pronounced [13–16]. In order to evaluate the performance of an emitter, the first step is typically the determination of the PLQY, followed by the measurement of the transient photoluminescence (PL) decay. Empirically, for TADF emitters the transient PL decay can then be fitted with a biexponential function $A_1\exp(-t/\tau_{PF})+A_2\exp(-t/\tau_{DF})$, with A_1, A_2, τ_{PF}, and τ_{DF} as fitting parameters. Here, τ_{PF} and τ_{DF} are the lifetimes of the prompt and delayed fluorescence, respectively, i.e, $\tau_{PF} < \tau_{DF}$. However, in order to obtain more quantitative information about kinetic processes, such as singlet radiative and nonradiative decay, intersystem crossing (ISC), and reverse ISC (RISC), the exciton kinetics are modeled numerically because coupled differential equations need to be solved to fully describe the singlet and triplet behavior. However, even with the rate constants of the various processes known, it is still difficult to directly evaluate the impact of the individual

[*]Corresponding authors: yungui.li@mpip-mainz.mpg.de
[†]blom@mpip-mainz.mpg.de

processes on the device performance [17–20]. In practice, after numerical modeling of the PL decays, OLEDs are fabricated and, to determine the CTP efficiency, the external quantum efficiency (EQE) is measured and compared with the calculated light outcoupling efficiency, which in turn also requires a number of optical input parameters that need to be experimentally determined. This series of numerical modeling and experimental steps makes the development of new efficient emitters a cumbersome process. It would be highly beneficial if the rate constants of the various excitonic processes as well as CTP efficiency could be directly determined from the PLQY and a biexponential fit of the transient PL decay only. Then not only could the OLED performance be directly predicted, but the effect of the various kinetic processes on OLED efficiency could also be quickly evaluated. However, analytical descriptions of the CTP efficiency with kinetic parameters related to singlet and triplet transitions in electroluminescent devices are still absent.

In the present study, analytical formulae for PLQY and CTP conversion efficiency for devices based on organic semiconducting materials have been derived in a unified manner for materials with different photophysical properties, i.e., with conventional fluorescence, phosphorescence, or TADF emission. Furthermore, combined with transient PL decay, based on the derived analytical description of exciton dynamics, the intrinsic kinetic rates and CTP conversion efficiency in devices can be estimated.

II. RESULTS AND DISCUSSION

A. Theoretical derivation

The derivation is based on a three-level model with a ground state, a singlet state, and a triplet state, in which nonradiative kinetic losses from singlets and triplets are treated separately. There are reports about higher lying triplet states being involved in efficient TADF emission, but here we only use the simplest model to derive the exciton kinetics [21]. As we demonstrate in the following sections, it turns out such a simple model can already explain many important photophysical properties for TADF emitters.

The exciton kinetics under pulsed excitation for singlets and triplets is schematically illustrated in Fig. 1, in which the initial exciton densities under PL or electroluminescence (EL) are indicated.

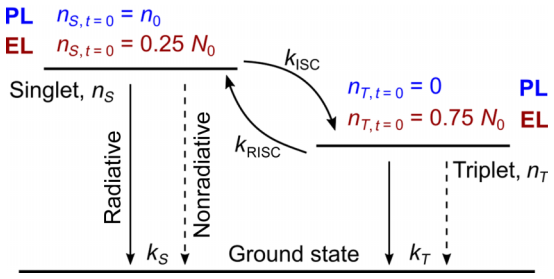

FIG. 1. Jablonski diagram for different types of organic emitters with a unified three-level model, consisting of a ground state, singlet state, and triplet excited state, with consideration of the spin-allowed and spin-flip processes. Initial exciton densities under photoluminescence (PL) or electroluminescence (EL) are indicated.

The exciton dynamics for singlets and triplets, intrinsically determined by the kinetic competition of fast spin-allowed and spin-flip transitions normally with a slower rate, can be described with the following rate equations in a unified matrix form [22,23]:

$$\frac{d}{dt}\begin{bmatrix} n_S \\ n_T \end{bmatrix} = \begin{bmatrix} -k_S - k_{\mathrm{ISC}} & k_{\mathrm{RISC}} \\ k_{\mathrm{ISC}} & -k_T - k_{\mathrm{RISC}} \end{bmatrix}\begin{bmatrix} n_S \\ n_T \end{bmatrix}. \quad (1)$$

In this equation, n_S is the singlet density and n_T the triplet density, k_S is the sum of the singlet radiative k_r^S and nonradiative rate k_{nr}^S, while k_{ISC} and k_{RISC} are the ISC and RISC rates, respectively. The triplet transition rate k_T includes both radiative and nonradiative relaxations.

Here, since we only consider the transient behavior for singlets and triplets, the generation term is omitted in Eq. (1) [24]. In such a case, we can treat the initial exciton densities generated either by photon (i.e., PL) or electrical (i.e., EL) pulses as the initial conditions for Eq. (1). There is no generation term in the transient case, which is different compared to steady-state excitation [24].

To solve this equation, in which nonlinear molecular interactions are not considered, one can calculate the eigenvalues (λ_1, λ_2) for the coefficient matrix of Eq. (1) as follows:

$$\lambda_1 = \frac{-(k_S + k_{\mathrm{ISC}} + k_{\mathrm{RISC}} + k_T) + \sqrt{(k_S + k_{\mathrm{ISC}} - k_{\mathrm{RISC}} - k_T)^2 + 4k_{\mathrm{ISC}}k_{\mathrm{RISC}}}}{2}, \quad (2a)$$

$$\lambda_2 = \frac{-(k_S + k_{\mathrm{ISC}} + k_{\mathrm{RISC}} + k_T) - \sqrt{(k_S + k_{\mathrm{ISC}} - k_{\mathrm{RISC}} - k_T)^2 + 4k_{\mathrm{ISC}}k_{\mathrm{RISC}}}}{2}. \quad (2b)$$

One can determine that $0<(-\lambda_1)<(-\lambda_2)$, $-(\lambda_1+\lambda_2)=(k_S+k_{\mathrm{ISC}}+k_{\mathrm{RISC}}+k_T)$, and $\lambda_1\lambda_2=(k_Sk_T+k_Sk_{\mathrm{RISC}}+k_Tk_{\mathrm{ISC}})$. Therefore, with two selected eigenvectors, the general solution for Eq. (1) is

$$\begin{bmatrix} n_S \\ n_T \end{bmatrix} = \begin{bmatrix} \lambda_1+k_{\mathrm{RISC}}+k_T & \lambda_2+k_{\mathrm{RISC}}+k_T \\ k_{\mathrm{ISC}} & k_{\mathrm{ISC}} \end{bmatrix} \begin{bmatrix} C_1e^{\lambda_1 t} \\ C_2e^{\lambda_2 t} \end{bmatrix}, \tag{3}$$

while constants C_1 and C_2 should be determined by the initial condition. Under PL excitation with the initial condition $n_S=n_0$ and $n_T=0$, one can obtain the analytical expression for singlet and triplet densities as a function of the relaxation time,

$$n_S^{\mathrm{PL}} = \frac{n_0(\lambda_1+k_{\mathrm{RISC}}+k_T)}{\lambda_1-\lambda_2}e^{\lambda_1 t} - \frac{n_0(\lambda_2+k_{\mathrm{RISC}}+k_T)}{\lambda_1-\lambda_2}e^{\lambda_2 t}, \tag{4a}$$

$$n_T^{\mathrm{PL}} = \frac{k_{\mathrm{ISC}}n_0}{\lambda_1-\lambda_2}(e^{\lambda_1 t}-e^{\lambda_2 t}). \tag{4b}$$

Therefore, in the transient case we are discussing here, the fraction of the integrated radiative singlets over the total generated singlets by the excitation pulse gives the PLQY for TADF emitters. The fluorescence PLQY, determined by the singlet radiative rate k_{r}^S, can be calculated as follows:

$$\eta_{\mathrm{PLQY}}^{\mathrm{fl}} = \frac{1}{n_0}\int_0^\infty k_{\mathrm{r}}^S n_S^{\mathrm{PL}}dt = \frac{k_{\mathrm{r}}^S(k_{\mathrm{RISC}}+k_T)}{k_Sk_T+k_Sk_{\mathrm{RISC}}+k_Tk_{\mathrm{ISC}}}. \tag{5}$$

Similarly, under PL excitation, the nonradiative quantum losses from singlets (η_{nr}^S) or triplets (η_{nr}^T) can be derived as Eqs. (A1) and (A2) in the Appendix. Experimentally, one would measure the PLQY by cw excitation under steady-state conditions. In such a case, the experimental PLQY is defined as the ratio of emitted photons to the total of absorbed photons within a specific duration. Therefore, Eq. (5) represents the description of PLQY in a kinetic manner, which can be experimentally measured by cw excitation, under the assumption that annihilation processes are absent during the measurement. In other words, the measured PLQY of TADF emitters under steady-state conditions is intrinsically determined by the kinetic rates given by Eq. (5).

For transient PL measurements with laser pulses as the excitation source, the intensity of each input pulse can be described by a Gaussian function with a full width at half maximum of t_0. In such a case, the initial exciton density n_0 is also time dependent on the laser intensity evolution. However, it should be noted that, for organic emitters, the singlet lifetime is normally in the nanosecond region. As a result, for pulsed lasers with a time resolution of hundreds of femtoseconds (10^{-13} s) or a few picoseconds (10^{-12} s), the time resolution of the excitation source is orders of magnitude lower than the decay lifetime. Therefore, for organic emitters excited by femtosecond or picosecond laser pulses, the initial exciton density can be reasonably treated as a constant value n_0.

Meanwhile, under electrical excitation with the initial condition $n_S=N_0/4$ and $n_T=3N_0/4$ for Eq. (3), in which N_0 is the total number of recombined excitons from charge-carrier pairs [25,26], we can then obtain the analytical description for singlet and triplet densities as follows:

$$n_S^{\mathrm{EL}} = \frac{N_0(\lambda_1+k_{\mathrm{RISC}}+k_T)(3\lambda_2-k_{\mathrm{ISC}}+3k_{\mathrm{RISC}}+3k_T)}{4(\lambda_2-\lambda_1)k_{\mathrm{ISC}}}e^{\lambda_1 t} + \frac{N_0(\lambda_2+k_{\mathrm{RISC}}+k_T)(k_{\mathrm{ISC}}-3\lambda_1-3k_{\mathrm{RISC}}-3k_T)}{4(\lambda_2-\lambda_1)k_{\mathrm{ISC}}}e^{\lambda_2 t}, \tag{6a}$$

$$n_T^{\mathrm{EL}} = \frac{N_0(3\lambda_2-k_{\mathrm{ISC}}+3k_{\mathrm{RISC}}+3k_T)}{4(\lambda_2-\lambda_1)}e^{\lambda_1 t} + \frac{N_0(k_{\mathrm{ISC}}-3\lambda_1-3k_{\mathrm{RISC}}-3k_T)}{4(\lambda_2-\lambda_1)}e^{\lambda_2 t}. \tag{6b}$$

Therefore, the analytical description for the CTP efficiency $\eta_{\mathrm{CTP}}^{\mathrm{fl}}$ based on TADF emission, can be described as follows:

$$\eta_{\mathrm{CTP}}^{\mathrm{fl}} = \frac{1}{N_0}\int_0^\infty k_{\mathrm{r}}^S n_S^{\mathrm{EL}}dt = k_{\mathrm{r}}^S\frac{(\lambda_1+k_{\mathrm{RISC}}+k_T)(3\lambda_2-k_{\mathrm{ISC}}+3k_{\mathrm{RISC}}+3k_T)}{4(\lambda_1-\lambda_2)k_{\mathrm{ISC}}\lambda_1} + k_{\mathrm{r}}^S\frac{(\lambda_2+k_{\mathrm{RISC}}+k_T)(k_{\mathrm{ISC}}-3\lambda_1-3k_{\mathrm{RISC}}-3k_T)}{4(\lambda_1-\lambda_2)k_{\mathrm{ISC}}\lambda_2}. \tag{7}$$

We note that Eq. (7) can be simplified for conventional fluorescence or phosphorescence emitters, derived as Eqs. (A3) and (A4) in the Appendix.

Here, similar to the PLQY of Eq. (5), Eq. (7) describes the CTP efficiency from a kinetic perspective. Since only the intrinsic exciton decay is considered, the trapping or annihilation behavior under EL excitation is omitted here. Therefore, the CTP conversion efficiency described by Eq. (7) is the theoretical maximum of the internal quantum efficiency for electroluminescent devices based on TADF emitters. Whenever there are losses from exciton trapping and/or annihilation, the experimental value should be lower than that predicted by Eq. (7).

In this derivation, each kinetic process involved is assumed with a constant rate. In the early stages, such a treatment was successfully applied to describe the photophysical properties of TADF systems [9]. Recently, there have been reports about the impact of different geometrical configurations on the triplet-state energy in donor-acceptor type TADF emitters [27]. From molecular simulations, when the dihedral angle between the donor and acceptor changes, the energy splitting between singlet and triplet states also varies, leading to a distribution of RISC rates. In the present study, which is focused on providing insight into the role of the kinetic processes on OLED performance, the ISC rate is assumed as a single value without considering the RISC rate distribution for clarity. Such a simplification indicates that all kinetic processes involved are dominated by a main rate.

Furthermore, from Eq. (4), for fluorescent and phosphorescent emitters, a simplified monoexponential decay behavior is predicted. Indeed, such decay has been experimentally observed for many organic emitters with only fluorescence emission, or phosphorescent emitters with heavy-atom effects [28]. Moreover, from Eqs. (3) and (4a), when assuming a constant RISC rate for TADF emitters, singlet relaxation can be described by Eq. (4) in the form of a biexponential function exhibiting prompt and delayed fluorescence decay, reported previously for many TADF emitters [17,29,30]. Therefore, the simplified model with a main rate for each kinetic process is a validated approximation to generally understand the excitonic kinetic behavior in organic emitters.

B. Numerical analysis

The singlet and triplet densities under PL excitation are numerically and analytically calculated and compared in Fig. 2. For the kinetic rates we have chosen a range that covers the typical reported rates for TADF emitters [31]. Symbols are densities simulated numerically with Eq. (1), while lines are densities calculated analytically with Eq. (4). Identical singlet densities have been obtained by numerical simulations and analytical formulae. For triplets, there are tiny differences close to time zero, which might result from the finite difference error of the numerical method. For longer delay times, the numerical and analytical results are identical for triplet densities as well.

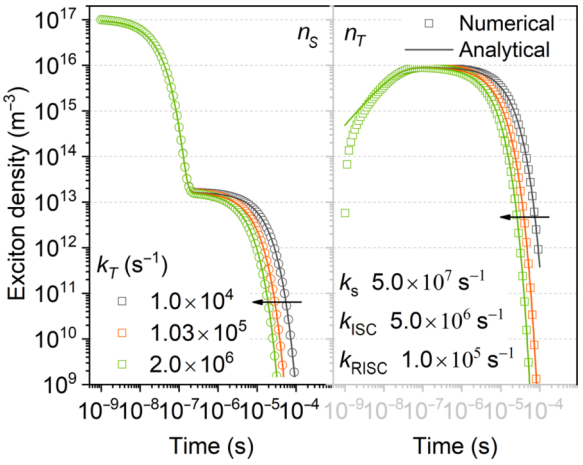

FIG. 2. Numerically and analytically calculated exciton densities for thermally activated delayed fluorescence (TADF) emitters under photoexcitation. Here, the initial singlet density n_0 is assumed as 1.0×10^{17} m^{-3}. Numerical simulations are done within the logarithmic time scale from 1.0×10^{-9} to 1.0×10^{-4} s with 1000 steps, with data points hidden for better visualization.

As shown in Fig. 2, when assuming $k_S = 5 \times 10^7$ s^{-1}, $k_{ISC} = 5 \times 10^6$ s^{-1}, and $k_{RISC} = 1.0 \times 10^5$ s^{-1}, the increase of the triplet relaxation rate k_T from 1.0×10^4 to 2.0×10^5 s^{-1} will gradually decrease the delayed fluorescence lifetime and its contribution to the total fluorescence. Since k_{ISC} and k_S are fixed, the prompt fluorescence decay in the nanosecond region is untouched.

The increase of the triplet relaxation rate k_T has significant impacts on the CTP efficiency at the device level. Based on these assumed kinetic parameters for the total singlet relaxation rate k_S (5×10^7 s^{-1}), ISC rate k_{ISC} (5×10^7 s^{-1}), and RISC rate k_{RISC} (1.0×10^5 s^{-1}), together with the tuned singlet radiative rate k_r^S and triplet nonradiative rate k_T, we can use the derived analytical formula Eq. (5) to calculate η_{PLQY}^{fl}. Furthermore, the CTP efficiency η_{CTP}^{fl} under EL excitation can be calculated with Eq. (7). As shown in Fig. 3, increasing the singlet radiative rate k_r^S will significantly increase the PLQY. In cases that nonradiative singlet loss is suppressed close to 0, i.e., $k_r^S \approx k_S$, the η_{PLQY}^{fl} can reach approximately 100%, even though the nonradiative triplet rate k_T is 2 times higher than k_{RISC} (1.0×10^5 s^{-1}). This is because the majority of the generated singlets can emit directly without singlet-triplet cycling, leading to limited triplet quantum loss η_{nr}^T.

A low singlet radiative rate k_r^S (e.g., 5×10^6 s^{-1}) indicates fast nonradiative relaxations ($k_S - k_r^S$) when the total singlet rate k_S is assumed as a fixed value (e.g., 5×10^7 s^{-1} here). In such a case, pronounced singlet nonradiative quantum loss η_{nr}^S occurs, giving rise to low PLQY or CTP efficiency, as shown in Fig. 3. Increasing the singlet radiative rate k_r^S (e.g., 5×10^6 s^{-1}) can suppress η_{nr}^S, therefore leading to a higher PLQY.

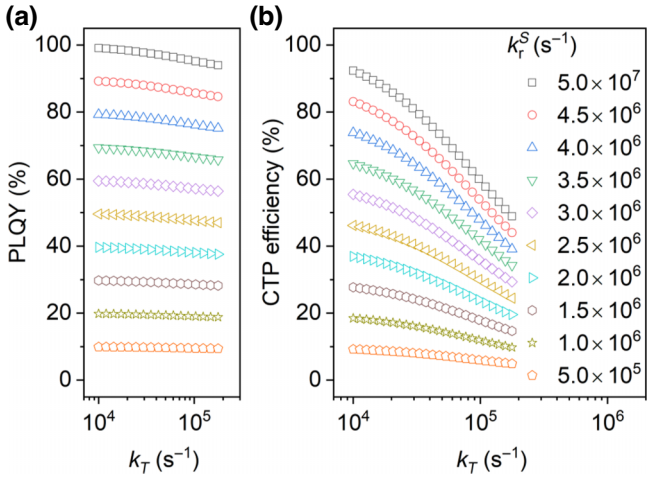

FIG. 3. Calculated photoluminescence quantum yield (PLQY) (a) and charge-to-photon (CTP) efficiency (b) for TADF emitters with different kinetic parameters based on derived analytical formulae, with $k_S = 5 \times 10^7$ s^{-1}, $k_{\mathrm{ISC}} = 5 \times 10^6$ s^{-1}, and $k_{\mathrm{RISC}} = 1.0 \times 10^5$ s^{-1}, while different singlet radiative rates k_r^S and triplet relaxation rates k_T are scanned. For TADF emitters, the triplet relaxation is treated as a nonradiative loss.

The ISC rate plays an important role as well. As shown in Fig. 4, when increasing k_{ISC} with a fixed singlet relaxation rate k_S, there is a gradual decrease of the prompt fluorescence lifetime, accompanied by an increased contribution of the delayed fluorescence. However, since the rates k_{RISC} and k_T are fixed, the triplet decay lifetime is maintained, though the maximum triplet density is changed.

Both PLQY and CTP efficiency are highly dependent on the ISC rate for TADF emitters. As shown in Fig. 5(a), close to unity PLQY can be obtained when there is no significant singlet nonradiative decay, i.e., $k_r^S \approx k_S$. However, because of the direct triplet nonradiative loss, the CTP efficiency can reach only around 70% in these cases when the ISC rate is 1 order lower than the total singlet relaxation rate k_S. Further increasing k_{ISC} to $1k_S$–$2k_S$ will reduce the CTP efficiency to around 40%–50% [Fig. 5(b)], with only a slight reduction of the PLQY to 60%–70% [Fig. 5(a)].

In real cases of TADF emitters, it is most likely that both singlet and triplet nonradiative losses are simultaneously present, i.e., $k_r^S < k_S$ and $k_T > 0$. As shown in Fig. 3(a), it is still possible to obtain a PLQY as high as around 90% in these cases with pronounced delayed fluorescence as presented in Fig. 2. TADF emitters with such high PLQYs and pronounced delayed fluorescence are intuitively treated as potential candidates for high-performance devices. However, the CTP efficiency highly depends on the ratio between k_{RISC} and k_T. Whenever the rate k_T is about $0.5k_{\mathrm{RISC}}$–$1k_{\mathrm{RISC}}$, the CTP efficiency will significantly reduce to only 50%–60%, shown in Fig. 3(b), as compared to the high PLQY around 90%. Considering the optical outcoupling efficiency of approximately 25% in EL devices [7] based on TADF emitters with such a high PLQY and pronounced delayed fluorescence, the maximum EQE can reach only around 12% at the device level. Such a quantitative analysis based on analytical formulae is consistent with the previous discussion based on numerical modeling [18]. It indicates that the precise quantification of nonradiative losses from triplets and singlets is of vital importance for TADF emitters.

C. Paradox of high PLQYs with low CTP efficiency

Having an analytical description for the CTP efficiency of OLEDs also enables us to clarify the counterintuitive

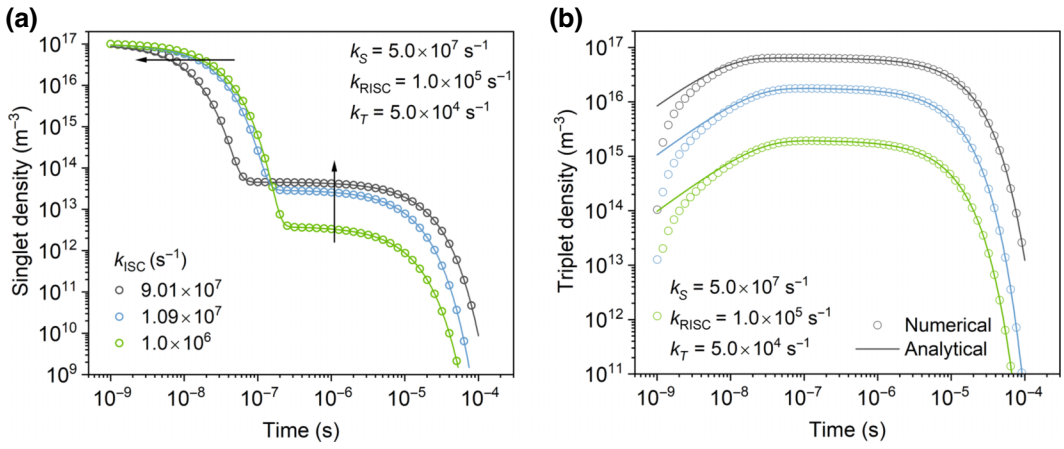

FIG. 4. Numerically and analytically calculated exciton densities for TADF emitters under photoexcitation. Here, the initial singlet density n_0 is assumed as 1.0×10^{17} m^{-3}, while the kinetics rates k_s, k_{ISC}, k_{RISC}, and k_T are assumed in ranges experimentally determined for many TADF emitters. (a) Singlet density and (b) triplet density. Numerical simulations are done within the time range from 1.0×10^{-9} to 1.0×10^{-4} s in a logarithmic scale with 1000 steps. Some data points are hidden in plots for better visualization.

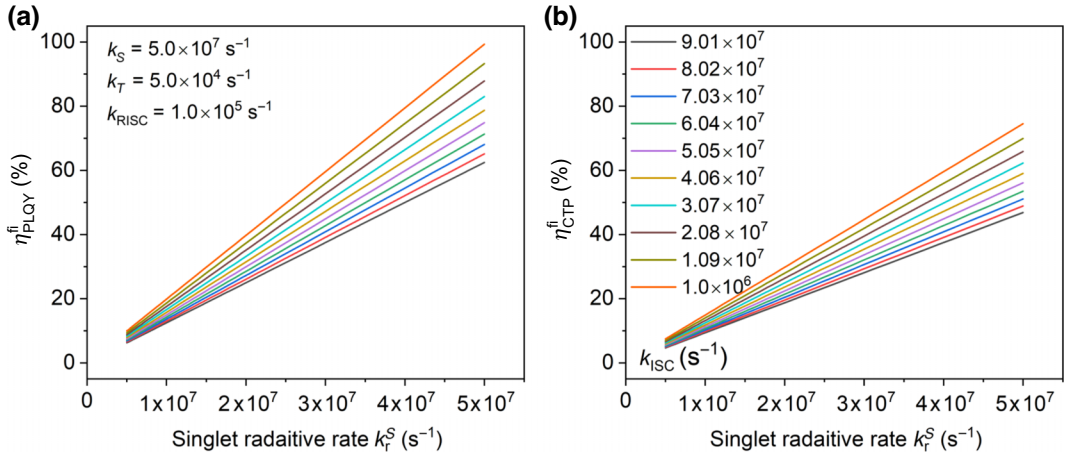

FIG. 5. Impacts of the ISC rate k_{ISC} and singlet radiative rate k_r^S on (a) PLQY and (b) CTP efficiency for TADF emitters with a fixed total singlet relaxation rate $k_S = 5 \times 10^7$ s^{-1}, calculated with the analytical formulae, with other kinetic parameters $k_{RISC} = 1 \times 10^5$ s^{-1} and $k_T = 5.0 \times 10^4$ s^{-1}.

simultaneous occurrence of TADF emitters with a high PLQY but low CTP efficiency in devices. We demonstrate that this apparent paradox can result from a subtle difference in k_{RISC} or k_T in these systems, though with similar rates of other kinetic processes.

To explain the phenomenon in more detail, we here consider two possible mechanisms: a change of k_{RISC} or a variation in k_T. We firstly assume TADF systems with high and identical PLQYs of 90%, with the following common kinetic rates: $k_S = 5 \times 10^7$ s^{-1}, $k_{ISC} = 5 \times 10^6$ s^{-1}, and $k_T = 5 \times 10^4$ s^{-1}, while k_r^S is varied from $0.01k_S$ to $1.0k_S$. With these kinetic rates, from Eq. (5), we can calculate the possible RISC rates to maintain the PLQY of 90%. A non-negative RISC rate is obtained when k_r^S is in the range (4.6–4.8) $\times 10^7$ s^{-1}. With these calculated kinetic rates, as shown in Fig. 6(b), the CTP efficiency changes significantly when the RISC rate is varied. In other words, for TADF systems with identical PLQY, the CTP efficiency can be very different depending on the RISC rate. Nevertheless, in this case, a very different transient PL decay is predicted by numerical modeling from Eq. (1), as shown in Fig. 6(a). The fitted τ_{PF} is identical for all different combinations of k_r^S and k_{RISC}, as shown in Fig. 6(c). However, the intensity and lifetime of the delayed fluorescence greatly changes, as shown in Figs. 6(a) and 6(c). As a result, when a large difference in CTP efficiency for two TADF emitters with nearly equal PLQY originates from a variation in k_{RISC}, this is typically reflected as a strong variation in the delayed fluorescence.

Alternatively, we discuss the case of TADF emitters with equal PLQY but with different nonradiative triplet decay rates. Additionally, here we assume TADF systems with identical PLQYs of 90% and with kinetic rates of $k_S = 5 \times 10^7$ s^{-1}, $k_{ISC} = 5 \times 10^6$ s^{-1}, and $k_{RISC} = 1 \times 10^5$ s^{-1}, while k_r^S is varied from $0.01k_S$ to $1.0k_S$. Similarly, with these kinetic rates, we can calculate the possible k_T to maintain a PLQY of 90% from Eq. (5). Using these kinetic parameters within the physically meaningful range, we then obtain the decay kinetics of singlets, as shown in Fig. 6(d). The fitted τ_{PF}, is identical for all different combinations of k_r^S and k_T as shown in Figs. 6(d) and 6(f). However, as shown in Fig. 6(e), the CTP efficiency in devices strongly decreases as k_T increases. The CTP efficiency is only 45%–75%, with k_r^S slightly changed from 4.6×10^7 to 4.8×10^7 s^{-1} and k_T from 2.8×10^4 to 2.0×10^5 s^{-1}. Remarkably, such a change of k_T results in only a relatively small variation of τ_{DF} from 3.4 to 8.4 μs, while the intensity of the delayed fluorescence is maintained, as shown in Fig. 6(d). Furthermore, the PLQY is not very sensitive to a small change of k_T [Fig. 3(a)]. Therefore, experimentally, it is possible to see a very different device efficiency in OLEDs based on apparently similar TADF systems with close PLQYs and similar transient PL decays. This apparent contradiction can be explained by a subtle difference in triplet kinetics, especially the triplet nonradiative decay.

D. Correlation with experimental results

Having set the analytical framework, we now demonstrate how it facilitates the evaluation of TADF emitters. First, the PLQY and transient PL decay are experimentally measured. As mentioned, the transient PL decay can be fitted with a biexponential function $A_1\exp(-t/\tau_{PF}) + A_2\exp(-t/\tau_{DF})$, with $\tau_{PF} < \tau_{DF}$. In combination with the measured PLQY, one can calculate all kinetic rates assuming a certain triplet nonradiative rate. A detailed derivation with analytical formulae has been done in the Appendix, Eqs. (A6)–(A13), with the full consideration of singlet and triplet nonradiative losses. However,

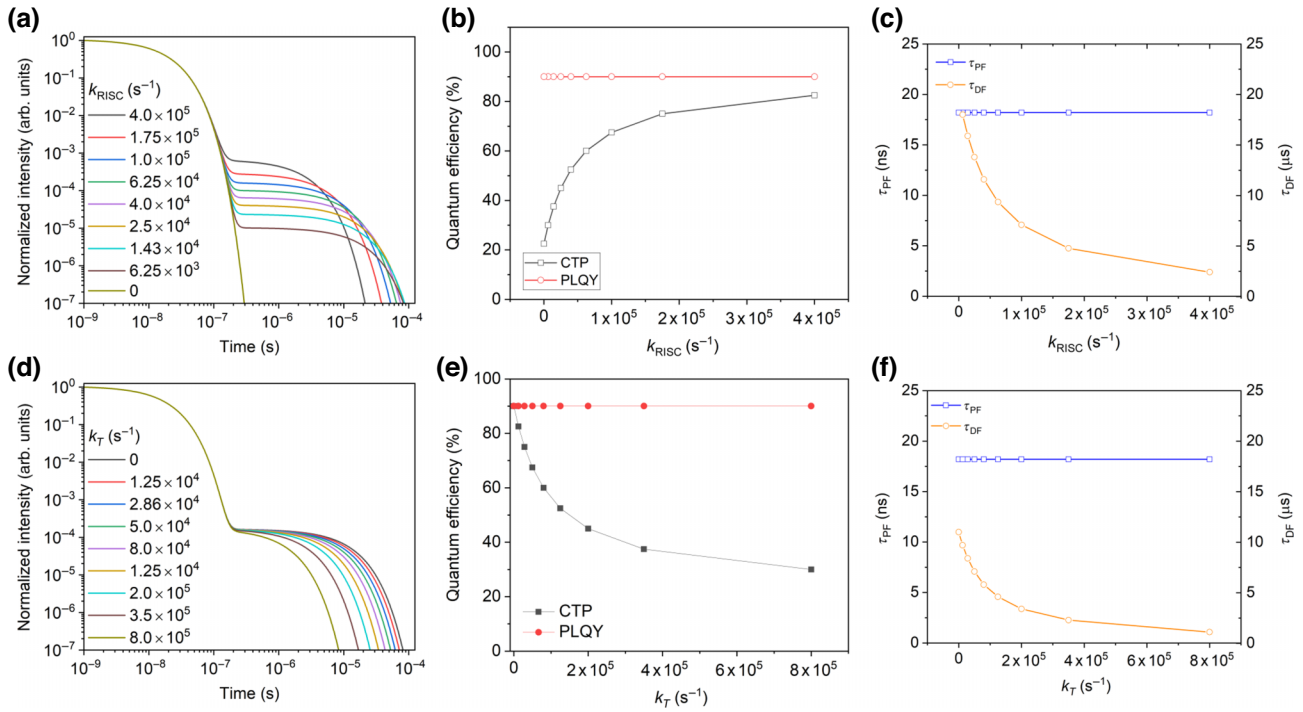

FIG. 6. The paradox of similar and high PLQYs with different and low CTP efficiencies in devices based on TADF emitters. Here, PLQY is assumed as 90%, k_S as 5×10^7 s^{-1}, and k_{ISC} as 5×10^6 s^{-1}, while k_r^S is varied from $0.01k_S$ to $1.0k_S$, together with changing k_{RISC} in (a)–(c) or k_T in (d)–(f) to maintain the constant PLQY. However, with the given rates, non-negative k_{RISC} or k_T can only be assured [Eq. (5)] when k_r^S is in a small range, roughly from $0.9k_S$ to $0.98k_S$, as indicated in the plots. (a),(d) Normalized singlet decay. (b),(e) PLQY and CTP efficiency. (c),(f) Fitted τ_{PF} and τ_{DF} from the singlet decay in (a),(d).

in efficient TADF emitters, the RISC rate (typically in the microsecond regime) is much faster than the spin-forbidden (nonradiative) triplet recombination (typically millisecond regime), such that nearly all triplets are recycled and triplet losses can be neglected. In other words, one can simplify these equations by only considering the singlet nonradiative process. In such a case, with $k_T = 0$, these equations simplify to

$$k_{RISC} = \frac{(A_2 - A_1)(\tau_{DF} - \tau_{PF})}{2\tau_{PF}\tau_{DF}} + \frac{\tau_{PF} + \tau_{DF}}{2\tau_{PF}\tau_{DF}}, \tag{8a}$$

$$k_r^S = \frac{\eta_{PLQY}^{fl}}{\tau_{PF}\tau_{DF}k_{RISC}}, \tag{8b}$$

$$k_{ISC} = \frac{(\tau_{DF} - \tau_{PF})/\tau_{PF}\tau_{DF}}{4k_{RISC}}, \tag{8c}$$

with

$$C = \frac{\tau_{PF} + \tau_{DF}}{2\tau_{PF}\tau_{DF}} - \frac{(A_2 - A_1)(\tau_{DF} - \tau_{PF})}{2\tau_{PF}\tau_{DF}}, \tag{8d}$$

and

$$k_S = C - k_{ISC}, \tag{8e}$$

$$k_{nr}^S = k_S - k_r^S. \tag{8f}$$

As a result, Eq. (8) can be directly used to estimate kinetic parameters using only the PLQY measurement and biexponential fitting of the PL decay, which is widely characterized for TADF systems. Furthermore, with these calculated kinetic rates we can then directly calculate the CTP efficiency for different TADF systems using Eq. (7). Therefore, the derived formulae allow us to directly determine the CTP efficiency in electroluminescent devices based only on the PLQY and biexponential PL decay without the need for any numerical calculations or device characterization.

E. Experimental verification

As an example, we here explain the detailed procedure to calculate kinetic rates and CTP efficiency based on the yellow TADF emitter CzDBA {9,10-bis[4-(9H-carbazol-9-yl)-2,6-dimethylphenyl]-9,10-diboraanthracene} [30]. The transient PL decay for the CzDBA neat film can be fitted with a biexponential decay function, with the fitting curve and fitting parameters shown in Fig. 7(a). Furthermore, the PLQY for a CzDBA neat film was reported previously as 90% [30]. Neglecting nonradiative triplet loss, the kinetic rate constants are then directly obtained from Eq. (8), resulting in a k_{ISC} of 1.0×10^6 s^{-1} and k_{RISC} of 2.7×10^5 s^{-1}. These analytically determined rates are very

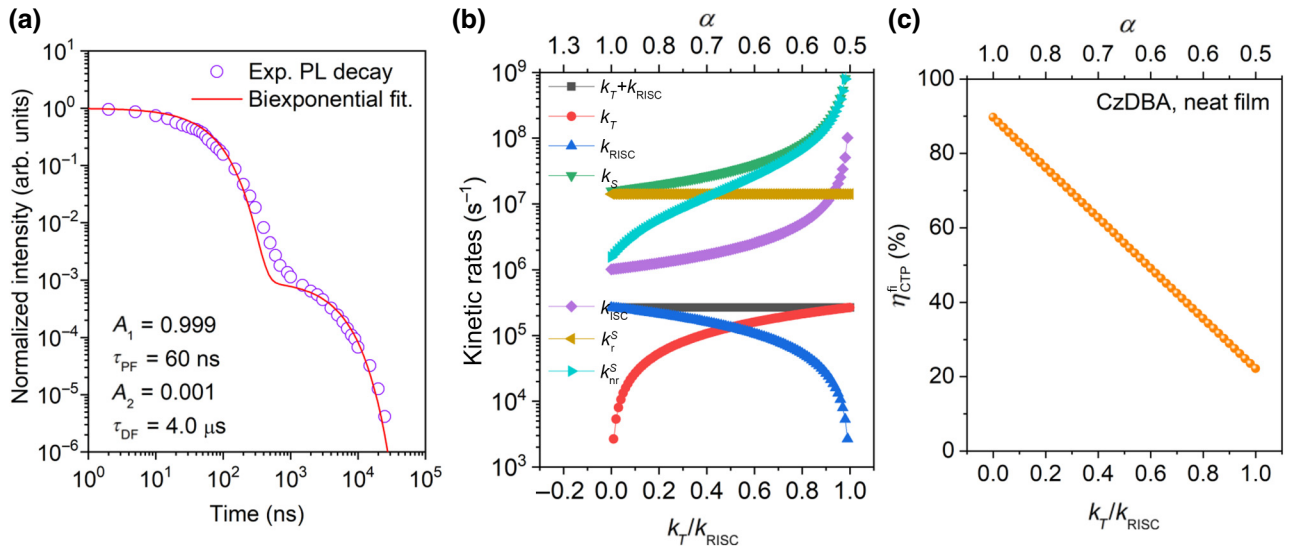

FIG. 7. Kinetic rates and CTP efficiency calculation based on experimental results of CzDBA neat film. (a) Biexponential fitting for the experimental transient PL decay reported in Ref. [17], with the fitting parameters shown. (b) Calculated kinetic parameters. (c) Calculated CTP efficiency for CzDBA neat film organic light-emitting diodes.

close to previously reported values for the same TADF system obtained from numerical modeling [17,28]. In this way, the relevant kinetic rates are quickly approximated.

To further evaluate the possible impact of nonradiative triplet recombination on the obtained rates, the more extensive Eq. (A6) can be used. Using the PLQY and the fitted τ_{PF} and τ_{DF} the sum of k_{RISC} and k_T can be calculated from Eq. (A6f). The singlet radiative rate k_r^S can be directly calculated using Eq. (A7). Then the contribution of the RISC rate k_{RISC} to the total triplet relaxation rate ($k_{RISC}+k_T$) can be varied, i.e., $\alpha = k_{RISC}/(k_{RISC}+k_T)$ in Eq. (A8a). Finally, the rest of kinetic parameters k_{ISC}, k_S, and k_{nr}^S can be calculated by Eqs. (A11)–(A13) sequentially as function of α. The obtained kinetic parameters for a CzDBA neat film are presented in Fig. 7(b).

We note that with minor triplet nonradiative contributions, meaning $0 < k_T/k_{RISC} < 0.2$, most calculated rates are relatively insensitive to the exact value of α. As a result, in most cases the simplified model [$k_T \approx 0$ and $\alpha \approx 1.0$, Eq. (8)] gives a very good quantification of the rates already.

With the above estimated kinetic rates, together with Eq. (7), we can further calculate the CTP efficiency, shown in Fig. 7(c), for devices based on a CzDBA neat film. The CTP efficiency is calculated to be around 80%–90% for α between 0.8 and 1.0. Previously, we have investigated CzDBA OLEDs experimentally. From EQE measurements (19%) and the modeling of the light outcoupling efficiency (25%) combined with a PLQY of 90%, the internal quantum efficiency for CzDBA OLEDs was estimated at around 85% [32]. The maximum internal quantum efficiency was obtained at a relatively low driving voltage (2.0–2.5 V), where bimolecular annihilation is not yet pronounced [33]. In such a case, the internal quantum efficiency approaches the CTP efficiency. Therefore, the CTP efficiency calculated with the derived formulae is consistent with the experimental results for CzDBA neat film OLEDs. We note that deviations of the biexponential decay behavior has also been observed for TADF emitters under high-power excitation due to bimolecular annihilation processes, which should be investigated by numerical modeling [17]. At low excitation power there is a close connection between the derived formulae and experimental results, which can be used to directly calculate key parameters including kinetic rates and CTP efficiency in electroluminescent devices.

We note that in previous works differential equations were numerically solved to obtain kinetic rates from PL decays, which is not straightforward [17,18]. In our approach, analytical formulae are derived to obtain all relevant rates with only the PLQY and the biexponential fitting parameters of transient PL as input parameters. Although similar analytical formulae based on kinetic models for TADF models have been derived previously, a direct link with OLED performance has not been obtained [22]. The direct link between a biexponential fit of the PL decay with device performance via analytical equations is of great benefit for the fast screening of the suitability of TADF emitters for OLEDs.

III. CONCLUSION

In summary, we have derived analytical formulae for the exciton densities and PLQY for organic emitters with three-level systems, with either conventional fluorescence, phosphorescence, or TADF emission in a unified manner.

Furthermore, the analytical expression of the charge-to-photon conversion efficiency in electroluminescent devices based on TADF emitters has been obtained. An example has been given to illustrate the procedure to calculate kinetic rates involved in a TADF system with derived analytical formulae and experimental results. Such a quantitative analysis based on analytical formulae makes it straightforward and handy to comprehensively understand the transient and steady-state photophysical properties of organic emitters and translate the results directly to device efficiencies, facilitating the further development of organic light-emitting devices.

APPENDIX

1. CTP efficiency for conventional fluorescence and phosphorescence emitters

For conventional fluorescence emitters, the triplet emission is negligible and the emission stems from singlets only, while the RISC process is absent because of the large ΔE_{ST}. With $k_{\mathrm{RISC}}=0$, we can determine that $\lambda_1=-k_T$, and $\lambda_2=-k_S-k_{\mathrm{ISC}}$. The CTP efficiency for conventional fluorescence emitters $\eta^{\star}_{\mathrm{CTP}}$ in devices can be simplified as follows:

$$\eta^{\star}_{\mathrm{CTP}}=\frac{k_{\mathrm{r}}^{S}}{4(k_S+k_{\mathrm{ISC}})}. \tag{A1}$$

It is consistent with previous demonstrations that the CTP efficiency for devices based on conventional fluorescence emitters can reach only a quarter of the PLQY, without the consideration of bimolecular annihilation-generated emission singlets.

For phosphorescence emitters, in which the emission comes only from triplets with fast ISC processes, k_{RISC} can be dropped together with a high k_{ISC} rate. Therefore, the analytical description for the maximum CTP efficiency for electroluminescent devices based on phosphorescence emitters is described as follows:

$$\begin{aligned}\eta^{\mathrm{ph}}_{\mathrm{CTP}}&=\frac{1}{N_0}\int_0^{\infty}k_{\mathrm{r}}^{T}n_T^{\mathrm{EL}}dt\\&=\frac{k_Tk_{\mathrm{ISC}}k_{\mathrm{r}}^{T}-k_{\mathrm{r}}^{T}(3k_S-4k_{\mathrm{ISC}}+3k_T)(k_S+k_{\mathrm{ISC}})}{4(k_S+k_{\mathrm{ISC}}-k_T)(k_S+k_{\mathrm{ISC}})k_T}.\end{aligned} \tag{A2}$$

For efficient phosphorescent emitters with heavy atoms such as iridium or osmium, in cases where $k_{\mathrm{ISC}}\gg k_S$ and $k_{\mathrm{ISC}}\gg k_T$, the CTP efficiency for devices based on phosphorescence emitters $\eta^{\mathrm{ph}}_{\mathrm{CTP}}$ can then be estimated by k_{r}^{T}/k_T.

2. Nonradiative losses

For fluorescent or TADF emitters, the triplet transition can be treated as a channel for the nonradiative loss, obtained as follows:

$$\eta_{\mathrm{nr}}^{T}=\frac{1}{n_0}\int_0^{\infty}k_Tn_T^{\mathrm{PL}}dt=\frac{k_Tk_{\mathrm{RISC}}}{k_Sk_T+k_Sk_{\mathrm{RISC}}+k_Tk_{\mathrm{ISC}}}, \tag{A3}$$

while the nonradiative loss from singlets, can be derived as follows:

$$\eta_{\mathrm{nr}}^{S}=1-\eta_{\mathrm{nr}}^{T}-\eta_{\mathrm{PLQY}}=\frac{k_{\mathrm{RISC}}(k_S-k_{\mathrm{r}}^{S})+k_T(k_S-k_{\mathrm{r}}^{S})}{k_Sk_T+k_Sk_{\mathrm{RISC}}+k_Tk_{\mathrm{ISC}}}. \tag{A4}$$

3. Combining derived formulae with experimental data to understand TADF photophysics

The derived analytical formula Eq. (6a) can be used to directly fit the transient photoluminescence decay for TADF emitters. In the normalized case, the initial exciton density n_0 in Eq. (4a) is cancelled, so only the related kinetic parameters impact the decay line shape, thus

$$I_{\mathrm{PL}}^{\mathrm{norm}}=\frac{(\lambda_1+k_{\mathrm{RISC}}+k_T)}{\lambda_1-\lambda_2}e^{\lambda_1 t}-\frac{(\lambda_2+k_{\mathrm{RISC}}+k_T)}{\lambda_1-\lambda_2}e^{\lambda_2 t}. \tag{A5}$$

Experimentally, the transient PL decay can be fitted with a biexponential decay function $A_1\exp(-t/\tau_{\mathrm{PF}})+A_2\exp(-t/\tau_{\mathrm{DF}})$, with A_1, A_2, τ_{PF}, and τ_{DF} being positive fitting parameters. Here, τ_{PF} and τ_{DF} are fitted lifetimes for the prompt fluorescence (PF) and delayed fluorescence (DF). Comparing with Eqs. (4a) and (A5), one can obtain

$$A_1=-\frac{\lambda_2+k_{\mathrm{RISC}}+k_T}{\lambda_1-\lambda_2}, \tag{A6a}$$

$$A_2=\frac{\lambda_1k_{\mathrm{RISC}}+k_T}{\lambda_1-\lambda_2}, \tag{A6b}$$

$$\tau_{\mathrm{PF}}=\frac{1}{-\lambda_2}, \tag{A6c}$$

$$\tau_{\mathrm{DF}}=\frac{1}{-\lambda_1}. \tag{A6d}$$

According to Eq. (A6), in such a biexponential fitting for transient PL decay, the sum of two prefactors A_1 and A_2 should be 1. In other words, Eqs. (A6a) and (A6b) are correlated, and they cannot be treated as two independent equations. To mitigate the fitting uncertainty that is normally observed with a biexponential fitting, from Eqs. (A6a) and (A6b), one can deduce that

$$k_{\mathrm{RISC}}+k_T=\frac{(A_2-A_1)(\lambda_1-\lambda_2)-(\lambda_1+\lambda_2)}{2}. \tag{A6e}$$

Equation (A6e) can be further written with fitting parameters τ_{PF} and τ_{DF}, according to Eqs. (A6c) and (A6d),

$$k_{\mathrm{RISC}}+k_T=\frac{(A_2-A_1)(\tau_{\mathrm{DF}}-\tau_{\mathrm{PF}})}{2\tau_{\mathrm{PF}}\tau_{\mathrm{DF}}}+\frac{\tau_{\mathrm{PF}}+\tau_{\mathrm{DF}}}{2\tau_{\mathrm{PF}}\tau_{\mathrm{DF}}}=B. \tag{A6f}$$

In other words, the sum of k_{RISC} and k_T, denoted by B, can be precisely determined with the transient photoluminescence measurement after a biexponential fitting. Together with the experimentally determined PLQY, kinetically described by Eq. (5) in the main text, one can firstly determine the singlet radiative rate unambiguously as follows:

$$k_{\mathrm{r}}^{S} = \eta_{\mathrm{PLQY}}^{\mathrm{fl}} \frac{k_S k_T + k_S k_{\mathrm{RISC}} + k_T k_{\mathrm{ISC}}}{k_{\mathrm{RISC}} + k_T} = \eta_{\mathrm{PLQY}}^{\mathrm{fl}} \frac{\lambda_1 \lambda_2}{B} = \frac{\eta_{\mathrm{PLQY}}^{\mathrm{fl}}}{\tau_{\mathrm{PF}} \tau_{\mathrm{DF}} B}. \tag{A7}$$

Assuming the contribution of the RISC rate among the sum of k_{RISC} and k_T, thus,

$$\frac{k_{\mathrm{RISC}}}{k_{\mathrm{RISC}} + k_T} = \alpha, \tag{A8a}$$

together with Eq. (A6f), we can then estimate the rates k_{RISC} and k_T, respectively, as follows:

$$k_{\mathrm{RISC}} = \alpha B, \tag{A8b}$$

$$k_T = (1-\alpha) B, \tag{A8c}$$

$$\frac{k_T}{k_{\mathrm{RISC}}} = \frac{1-\alpha}{\alpha}. \tag{A8d}$$

When there is no triplet nonradiative decay, α approaches 1. According to Eq. (2), it is known that $(\lambda_1 + \lambda_2) = -(k_S + k_{\mathrm{ISC}} + k_{\mathrm{RISC}} + k_T)$. We can determine the sum of k_S and k_{ISC} as C,

$$k_S + k_{\mathrm{ISC}} = -(\lambda_1 + \lambda_2) - (k_{\mathrm{RISC}} + k_T) = \frac{\tau_{\mathrm{PF}} + \tau_{\mathrm{DF}}}{2\tau_{\mathrm{PF}}\tau_{\mathrm{DF}}} - \frac{(A_2 - A_1)(\tau_{\mathrm{DF}} - \tau_{\mathrm{PF}})}{2\tau_{\mathrm{PF}}\tau_{\mathrm{DF}}} = C. \tag{A9}$$

Furthermore, according to Eq. (2), one can derive that

$$\lambda_1 - \lambda_2 = \sqrt{(k_S + k_{\mathrm{ISC}} - (k_{\mathrm{RISC}} + k_T))^2 + 4 k_{\mathrm{ISC}} k_{\mathrm{RISC}}}. \tag{A10a}$$

Together with Eqs. (A6) and (A9), one can rewrite Eq. (A10a) with the only unknown parameter k_{ISC} as follows:

$$\frac{\tau_{\mathrm{DF}} - \tau_{\mathrm{PF}}}{\tau_{\mathrm{PF}}\tau_{\mathrm{DF}}} = \sqrt{(C-B)^2 + 4 k_{\mathrm{ISC}} \alpha B}, \tag{A10b}$$

with B and C described by Eqs. (A6f) and (A9). Afterwards, one can then calculate k_{ISC} by solving Eq. (A10b), as follows:

$$k_{\mathrm{ISC}} = \frac{(\tau_{\mathrm{DF}} - \tau_{\mathrm{PF}}/\tau_{\mathrm{PF}}\tau_{\mathrm{DF}})^2 - (C-B)^2}{4\alpha B}. \tag{A11}$$

Furthermore, one can calculate the total singlet relaxation rate k_S from Eqs. (A9) and (A11) as follows:

$$k_S = C - k_{\mathrm{ISC}} = C - \frac{(\tau_{\mathrm{DF}} - \tau_{\mathrm{PF}}/\tau_{\mathrm{PF}}\tau_{\mathrm{DF}})^2 - (C-B)^2}{4\alpha B}. \tag{A12}$$

In the end, one can determine the singlet nonradiative rate k_{nr}^{S} from Eqs. (A12) and (A7),

$$k_{\mathrm{nr}}^{S} = k_S - k_{\mathrm{r}}^{S} = C - \frac{(\tau_{\mathrm{DF}} - \tau_{\mathrm{PF}}/\tau_{\mathrm{PF}}\tau_{\mathrm{DF}})^2 - (C-B)^2}{4\alpha B} - \frac{\eta_{\mathrm{PLQY}}^{\mathrm{fl}}}{\tau_{\mathrm{PF}}\tau_{\mathrm{DF}} B}, \tag{A13}$$

with B and C described by Eqs. (A6f) and (A9) with experimentally determined parameters.

In summary, from the PLQY and biexponential fitting of a TADF system, with the assumption about the triplet nonradiative contribution, i.e., α in Eq. (A8a), one can then further determine all kinetic parameters involved in the specific TADF system. With these kinetic parameters, it is then possible to calculate the CTP efficiency in electroluminescent devices with Eq. (7).

[1] A. Hepp, H. Heil, W. Weise, M. Ahles, R. Schmechel, and H. von Seggern, Light-emitting field-effect transistor based on a tetracene thin film, Phys. Rev. Lett. **91**, 157406 (2003).

[2] Q. Pei, G. Yu, C. Zhang, Y. Yang, and A. J. Heeger, Polymer light-emitting electrochemical cells, Science **269**, 1086 (1995).

[3] C. W. Tang and S. A. Vanslyke, Organic electroluminescent diodes, Appl. Phys. Lett. **51**, 913 (1987).

[4] W. F. Pasveer, J. Cottaar, C. Tanase, R. Coehoorn, P. A. Bobbert, P. W. M. Blom, D. M. de Leeuw, and M. A. J. Michels, Unified description of charge-carrier mobilities in disordered semiconducting polymers, Phys. Rev. Lett. **94**, 206601 (2005).

[5] P. W. M. Blom and M. C. J. M. Vissenberg, Dispersive hole transport in poly(*p*-phenylene vinylene), Phys. Rev. Lett. **80**, 3819 (1998).

[6] Y. Zhang and S. R. Forrest, Triplets contribute to both an increase and loss in fluorescent yield in organic light emitting diodes, Phys. Rev. Lett. **108**, 267404 (2012).

[7] B. Van der Zee, Y. Li, G. A. H. Wetzelaer, and P. W. M. Blom, Efficiency of polymer light-emitting diodes: A perspective, Adv. Mater. **34**, 2108887 (2022).

[8] M. Thompson, The evolution of organometallic complexes in organic light-emitting devices, MRS Bull. **32**, 694 (2007).

[9] F. B. Dias, T. J. Penfold, and A. P. Monkman, Photophysics of thermally activated delayed fluorescence molecules, Methods Appl. Fluoresc. **5**, 012001 (2017).
[10] H. Uoyama, K. Goushi, K. Shizu, H. Nomura, and C. Adachi, Highly efficient organic light-emitting diodes from delayed fluorescence, Nature **492**, 234 (2012).
[11] N. Aizawa, Y. Pu, Y. Harabuchi, A. Nihonyanagi, R. Ibuka, H. Inuzuka, B. Dhara, Y. Koyama, K. Nakayama, S. Maeda, F. Araoka, and D. Miyajima, Delayed fluorescence from inverted singlet and triplet excited states, Nature **609**, 502 (2022).
[12] M. A. Baldo, D. F. O'Brien, Y. You, A. Shoustikov, S. Sibley, M. E. Thompson, and S. R. Forrest, Highly efficient phosphorescent emission from organic electroluminescent devices, Nature **395**, 151 (1998).
[13] Y. Li, L. Jiang, W. Liu, S. Xu, T. Li, F. Fries, O. Zeika, Y. Zou, C. Ramanan, S. Lenk, R. Scholz, D. Andrienko, X. Feng, K. Leo, and S. Reineke, Reduced intrinsic non-radiative losses allow room-temperature triplet emission from purely organic emitters, Adv. Mater. **33**, 2101844 (2021).
[14] S. Yin, Q. Peng, Z. Shuai, W. Fang, Y.-H. Wang, and Y. Luo, Aggregation-enhanced luminescence and vibronic coupling of silole molecules from first principles, Phys. Rev. B **73**, 205409 (2006).
[15] J. Mei, N. L. C. Leung, R. T. K. Kwok, J. W. Y. Lam, and B. Z. Tang, Aggregation-induced emission: Together we shine, united we soar!, Chem. Rev. **115**, 11718 (2015).
[16] K. Tuong Ly, R. W. Chen-Cheng, H. W. Lin, Y. J. Shiau, S. H. Liu, P. T. Chou, C. S. Tsao, Y. C. Huang, and Y. Chi, Near-infrared organic light-emitting diodes with very high external quantum efficiency and radiance, Nat. Photonics **11**, 63 (2017).
[17] K. Thakur, B. Zee, G. A. H. Wetzelaer, C. Ramanan, and P. W. M. Blom, Quantifying exciton annihilation effects in thermally activated delayed fluorescence materials, Adv. Opt. Mater. **10**, 2101784 (2022).
[18] S. Sem, S. Jenatsch, K. Stavrou, A. Danos, A. P. Monkman, and B. Ruhstaller, Determining non-radiative decay rates in TADF compounds using coupled transient and steady state optical data, J. Mater. Chem. C **10**, 4878 (2022).
[19] S. Reineke, K. Walzer, and K. Leo, Triplet-exciton quenching in organic phosphorescent light-emitting diodes with Ir-based emitters, Phys. Rev. B **75**, 125328 (2007).
[20] M. A. Baldo, C. Adachi, and S. R. Forrest, Transient analysis of organic electrophosphorescence. II. Transient analysis of triplet-triplet annihilation, Phys. Rev. B **62**, 10967 (2000).
[21] T. Kobayashi, A. Niwa, K. Takaki, S. Haseyama, T. Nagase, K. Goushi, C. Adachi, and H. Naito, Contributions of a higher triplet excited state to the emission properties of a thermally activated delayed-fluorescence emitter, Phys. Rev. Appl. **7**, 1 (2017).
[22] Y. Tsuchiya, S. Diesing, F. Bencheikh, Y. Wada, P. L. dos Santos, H. Kaji, E. Zysman-Colman, I. D. W. Samuel, and C. Adachi, Exact solution of kinetic analysis for thermally activated delayed fluorescence materials, J. Phys. Chem. A **125**, 8074 (2021).
[23] R. Scholz, P. Kleine, R. Lygaitis, L. Popp, S. Lenk, M. K. Etherington, A. P. Monkman, and S. Reineke, Investigation of thermally activated delayed fluorescence from a donor–acceptor compound with time-resolved fluorescence and density functional theory applying an optimally tuned range-separated hybrid functional, J. Phys. Chem. A **124**, 1535 (2020).
[24] B. van der Zee, Y. Li, G. A. H. Wetzelaer, and P. W. M. Blom, Numerical device model for organic light-emitting diodes based on thermally activated delayed fluorescence, Adv. Electron. Mater. **8**, 2101261 (2022).
[25] P. W. M. Blom, M. J. M. De Jong, and S. Breedijk, Temperature dependent electron-hole recombination in polymer light-emitting diodes, Appl. Phys. Lett. **71**, 930 (1997).
[26] M. Kuik, G.-J. A. H. Wetzelaer, H. T. Nicolai, N. I. Craciun, D. M. De Leeuw, and P. W. M. Blom, 25th anniversary article: Charge transport and recombination in polymer light-emitting diodes, Adv. Mater. **26**, 512 (2014).
[27] W. Qiu, D. Liu, M. Li, X. Cai, Z. Chen, Y. He, B. Liang, X. Peng, Z. Qiao, J. Chen, W. Li, J. Pu, W. Xie, Z. Wang, D. Li, Y. Gan, Y. Jiao, Q. Gu, and S.-J. Su, Confining donor conformation distributions for efficient thermally activated delayed fluorescence with fast spin-flipping, Nat. Commun. **14**, 2564 (2023).
[28] J. R. Lakowicz, *Principles of Fluorescence Spectroscopy*, 3rd ed. (New York, Springer, 2006).
[29] Z. Huang, H. Xie, J. Miao, Y. Wei, Y. Zou, T. Hua, X. Cao, and C. Yang, Charge transfer excited state promoted multiple resonance delayed fluorescence emitter for high-performance narrowband electroluminescence, J. Am. Chem. Soc. **145**, 12550 (2023).
[30] T.-L. Wu, M.-J. Huang, C.-C. Lin, P.-Y. Huang, T.-Y. Chou, R.-W. Chen-Cheng, H.-W. Lin, R.-S. Liu, and C.-H. Cheng, Diboron compound-based organic light-emitting diodes with high efficiency and reduced efficiency roll-off, Nat. Photonics **12**, 235 (2018).
[31] M. Y. Wong and E. Zysman-Colman, Purely organic thermally activated delayed fluorescence materials for organic light-emitting diodes, Adv. Mater. **29**, 1605444 (2017).
[32] Y. Li, N. B. Kotadiya, B. Zee, P. W. M. Blom, and G. A. H. Wetzelaer, Optical outcoupling efficiency of organic light-emitting diodes with a broad recombination profile, Adv. Opt. Mater. **9**, 2001812 (2021).
[33] B. Zee, Y. Li, G. A. H. Wetzelaer, and P. W. M. Blom, Origin of the efficiency roll-off in single-layer organic light-emitting diodes based on thermally activated delayed fluorescence, Adv. Opt. Mater. **9**, 2100249 (2021).